Dalton Transactions

Accepted Manuscript

ROYAL SOCIETY OF CHEMISTRY

www.rsc.org/dalton

Cytotoxic Properties of a New Organometallic Platinum(II) Complex and its Gold(I) Heterobimetallic Derivatives

Maria Serratrice,[a] Laura Maiore,[a] Antonio Zucca,[a,b] Sergio Stoccoro,[a,b] Ida Landini,[c] Enrico Mini,[c] Lara Massai,[d] Giarita Ferraro,[e] Antonello Merlino,[e,f] Luigi Messori*[d] and Maria Agostina Cinellu,*[a,b]

[a]*Department of Chemistry and Pharmacy, University of Sassari, via Vienna 2, 07100 Sassari, Italy. E-mail: cinellu@uniss.it*
[b]*CIRCC, Consorzio Interuniversitario Reattività Chimica e Catalisi, Università di Bari, Via Celso Ulpiani 27, 70126 Bari, Italy*
[c]*Department of Health Sciences, Section of Clinical Pharmacology and Oncology, University of Florence, viale Pieraccini 6, 50139 Firenze, Italy*
[d]*Laboratory of Metals in Medicine, Department of Chemistry, University of Florence, via della Lastruccia 3, 50019 Sesto Fiorentino, Florence, Italy. E-mail: luigi.messori@unifi.it*
[e]*Department of Chemical Sciences, University of Naples Federico II, via Cintia, 80126, Napoli, Italy.*
[f]*CNR Institute of Biostructures and Bioimges, Via Mezzocannone 16, 80100, Napoli, Italy.*

Abstract

A novel platinum(II) organometallic complex, [Pt(pbi)(Me)(DMSO)], bearing the 2-(2′-pyridyl)-benzimidazole (pbiH) ligand, was synthesized and fully characterized. Interestingly, the reaction of this organometallic platinum(II) complex with two distinct gold(I) phosphane compounds afforded the corresponding heterobimetallic derivatives with the pbi ligand bridging the two metal centers. The antiproliferative properties *in vitro* of [Pt(pbi)(Me)(DMSO)] and its gold(I) derivatives as well as those of the known coordination platinum(II) and palladium(II) complexes with the same ligand, of general formula [MCl_2(pbiH)], were comparatively evaluated against A2780 cancer cells, either sensitive or resistant to cisplatin. A superior biological activity of the organometallic compound clearly emerged compared to the corresponding platinum(II) complex; the antiproliferative effects are further enhanced upon attaching the gold(I) triphenylphosphine moiety to the organometallic Pt compound. Remarkably, these novel metal species are able to overcome nearly completely resistance to cisplatin. Significant mechanistic insight on the study compounds was gained afterward upon investigating their reactions with a few representative biomolecules by electrospray mass spectrometry and X-ray crystallography. The obtained results are comprehensively discussed.

Introduction

Cisplatin and its second-generation analogues, carboplatin and oxaliplatin, are used worldwide for the clinical management of a variety of cancers, including: bladder, testicular, ovarian, head and neck, and lung cancers.[1] Three additional congeners of cisplatin, *i.e.* nedaplatin, lobaplatin and heptaplatin, were regionally approved for clinical use in Japan, China and Korea, respectively. However, the clinical effectiveness of cisplatin and - to some extent- of its analogues, is often limited by severe toxic side-effects, due to the rather poor ability of Pt drugs to distinguish between malignant and normal cells, as well as to the frequent occurrence of intrinsic and acquired cancer resistance to platinum.[2] Such severe drawbacks have spurred researchers to look for alternatives, both in the frame of platinum-based compounds[3] and in that of other transition metal derivatives.[4] Over the last 50 years, a plethora of platinum-based compounds were indeed prepared and screened as candidate antitumor agents. Many variations on the theme were proposed breaking one or more of the early established canonical rules of anticancer Pt drugs – *i.e.* oxidation state +2 of the Pt center, two ammine or amine donor groups and two anionic leaving groups in a *cis* geometry – leading to platinum(IV) complexes,[5] *trans*-platinum(II) complexes,[6] monofunctional platinum(II) complexes[7] and other "non classical" structures. In addition to mononuclear, also a few multinuclear platinum(II) complexes were successfully developed.[8] The basic idea behind this strategy is that totally different structures from those of cisplatin and its analogues might provide the opportunity of identifying new antitumor drugs with a radically different mechanism of action.[9] Nevertheless, in spite of the variety of molecular mechanisms displayed by the different classes of platinum complexes, almost invariantly nuclear DNA turned out to be the main target for most of them with the consequence that resistance processes are often activated after prolonged exposure to Pt drugs. For the above mentioned reasons, in order to broaden the spectrum of activity, many researchers focused attention on the potential of anticancer drugs containing non-platinum metal centers.[4] Among them, ruthenium-[10] and gold-based[11] drugs were shown to be a promising alternative or, at least, to be complementary to platinum(II) anticancer drugs. Based on the latter possibility, *i.e.* the cooperation and/or synergism between a Pt-based drug and a cytotoxic non-Pt metal species, a number of mixed Pt/M systems were developed as well, featuring in some cases improved chemico-physical properties and, more interestingly, targeting different biological molecules.[12,13]

Within this frame, we decided to develop a new heterodimetallic combination based on Pt(II) and Au(I) by exploiting the great versatility of 2-(2′-pyridyl)-benzimidazole (pbiH) as a potential bridging ligand. A series of mono- and binuclear Au^{I} and Au^{III} complexes of this ligand, showing very promising anticancer properties, were recently reported by us.[14] An in depth study of

the electronic structures of these compounds revealed interesting structure/activity relationships.[15] Furthermore, the biological properties of various pbiH metal complexes *e.g.* [M(pbiH)Cl_2] (with M being either Pd or Pt) and of related compounds have been the subject of various studies. These metal complexes were tested, *inter alia*, against a variety of cancer cell lines, including fibroblast and brain tumors,[16] human RD Rhabdomyosarcoma,[17] HeLa-229 and A2780 both sensitive and resistant to cisplatin,[18] showing on the whole a rather modest inhibition. In the light of the poor performances of the Pt(II) complex as a potential anticancer agent, and moving in the framework of the so-called "rule breaking" cytotoxic platinum agents [19] we developed an organometallic version of the above complex, namely [Pt(pbi)(Me)(DMSO)]. Indeed, organometallic compounds, *i.e.* metal complexes containing at least one direct, covalent metal-carbon bond, were recently found to be promising anticancer drug candidates.[20]

Moreover, by using this latter species as a metallo-ligand, we could obtain heterodinuclear platinum(II)-gold(I) complexes. All these new metal complexes, as well as the known platinum(II) and palladium(II) adducts, have been tested for their antiproliferative activities *in vitro* in A2780 cancer cells, both sensitive and resistant to cisplatin. Results are compared with those obtained for analogous and parent gold complexes.

In addition the interactions of the new metal species with some model biomolecular targets were explored mainly through ESI MS and X-ray diffraction and valuable information gained on the resulting adducts and the inherent reactivity.

Results and Discussion

Synthesis and characterization of the complexes

The ligand 2-(2'-pyridil) benzimidazole (pbiH) was synthesized by condensation of pyridine-2-carboxylic acid and 1,2-phenylenediamine in the presence of polyphosphoric acid at 180 °C, according to a literature method.[21] The palladium complex [$PdCl_2$(pbiH)], **1**, was prepared by reaction of the ligand with the stoichiometric amount of Na_2PdCl_4 in refluxing ethyl alcohol according to a literature method,[18] while the platinum complex [$PtCl_2$(pbiH)], **2**, was synthesized by reaction of pbiH and [$PtCl_2(DMSO)_2$] in dichloromethane solution. Both compounds **1** and **2** are neutral and both feature the ligand in its protonated form, as stated by FT-IR and ^{1}H NMR data which are in accordance with those reported in the literature for these compounds.[16,17,18]

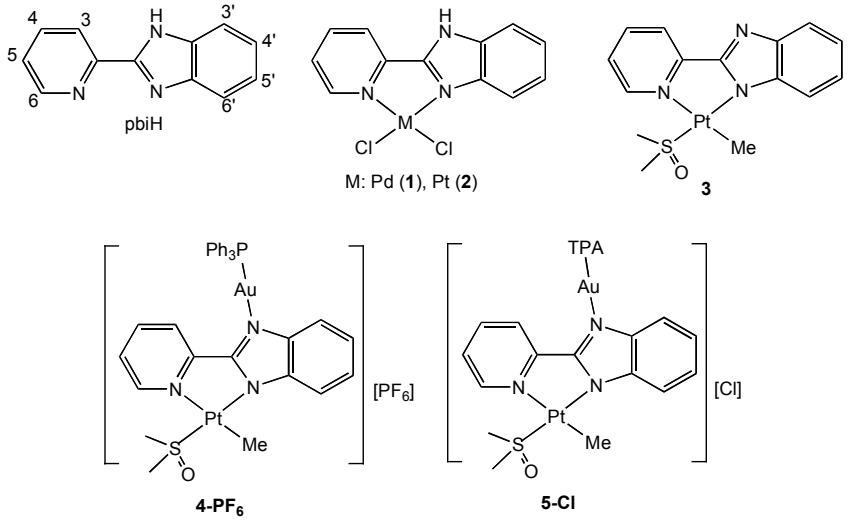

Scheme 1 Chemical structures of the ligand (with numbering scheme) and complexes

Under the same reaction conditions employed for the synthesis of **2**, the platinum(II) precursor $[Pt(Me)_2(DMSO)_2]$[22] afforded the neutral organometallic derivative [Pt(pbi)(Me)(DMSO)], **3**, as a yellow solid. This compound is soluble in most of the organic solvents and displays a high thermal stability (Mp 393 °C). At variance with compounds **1** and **2**, in complex **3** the Pt centre coordinates the pbi ligand through one iminic nitrogen of the pyridine ring and the deprotonated aminic nitrogen of the imidazole ring. Accordingly, the ^{1}H NMR spectrum shows the absence in the high frequencies region of any resonance attributable to the NH proton (*e.g.* at δ 13.53 ppm in **2**). In the absence of X-ray structural data, complex **3** was characterised in solution by means of bidimensional NMR spectroscopy, namely H–H COSY and H–H NOESY experiments. The COSY spectrum allowed assignment of all ^{1}H pbi resonances and the NOESY spectrum gave structural information. In particular the NOESY spectrum showed a NOE cross-peak between the Pt-CH_3, at 1.16 ppm, and the $H^{3'}$ proton (δ 7.77 ppm), thus indicating that of the two possible geometrical isomers the only formed was that one with the methyl ligand *trans* to the imino nitrogen of the pyridine ring (Fig. 1), in accordance to the higher *trans*-influence of the deprotonated amino nitrogen with respect to the imino one. A NOE cross-peak is also observed between the Pt-Me signal and that of the methyl protons of the coordinated DMSO ligand, at 3.34 ppm.

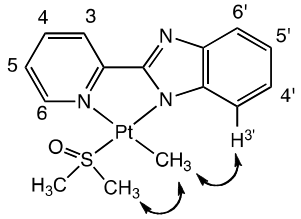

Fig. 1 Complex **3**: NOE contacts revealed by NOESY cross-peaks

The Pt-Me signal at δ 1.16 ppm is flanked by satellites with $^{2}J_{Pt-H}$ of 78.8 Hz; also coupled to ^{195}Pt is the signal of the methyl protons of the coordinated DMSO, with $^{3}J_{Pt-H}$ of 32.4 Hz. The H^{6} signal (δ 9.50 ppm) is strongly de-shielded with respect to the free ligand (Δδ = 0.86 ppm), and coupled to platinum ($^{3}J_{Pt-H}$ = 21.2 Hz); also downfield shifted is $H^{3'}$ (Δδ = 0.28 ppm), being in this complex in proximity of the coordinated nitrogen. At variance, the signals of H^{3}, $H^{4'}$/$H^{5'}$ and $H^{6'}$ are shifted at higher fields.

Reactions of compound **3**, acting as a metallo-ligand, with an equimolar amount of [Au(Ph_3P)][PF_6] (generated *in situ*) or of [AuCl(TPA)] (TPA = 1,3,5-triazaphosphaadamantane) afforded the hetero-binuclear compounds [(PPh_3)Au(μ-pbi)Pt(Me)(DMSO)][PF_6], **4-PF_6**, and [(TPA)Au(μ-pbi)Pt(Me)(DMSO)]Cl, **5-Cl**, respectively (Scheme 1). The ^{1}H NMR spectrum of **4-PF_6** in $CDCl_3$ solution shows the signals of the methyl protons at δ 1.20 (Pt-Me) and 3.42 ppm (Me_2SO) flanked by satellites with Pt-H coupling constants of 73.2 and 30.4 Hz, respectively, thus ruling out any transmetalation or ligand exchange reaction with the coordinatively unsatured {(PPh_3)Au^{+}} moiety. The latter is coordinated to the imino imidazole nitrogen, as shown by the broadening of the H^{3} proton of the pyridine ring; all the pyridine protons are downfield shifted with respect to the parent compound **3**. The $^{31}P\{^{1}H\}$ NMR spectrum further confirms the coordination of PPh_3 to gold(I): indeed, both the chemical shift of the phosphine (33.2 ppm) and the absence of satellites ruled out the possibility of coordination to platinum(II).[23] In the case of compound **5-Cl**, the ^{1}H NMR spectrum in acetone-d_6 shows, also in this case, the signals of the methyl protons at δ 1.26 (Pt-Me) and 3.54 ppm (Me_2SO) flanked by satellites with $^{2}J_{Pt-H}$ = 79.2 Hz and $^{3}J_{Pt-H}$ = 32.8 Hz, respectively. The N-CH_2-N protons of the TPA ligand give rise to an AB spin system centred at δ 4.59 ppm (J_{AB} = 12.2 Hz) and the N-CH_2-P a singlet resonance at δ 4.44 ppm. Also in this complex the H^{6} proton is the most deshielded (δ 9.67 ppm) and coupled to ^{195}Pt ($^{3}J_{Pt-H}$ = 19.2 Hz). The ^{31}P NMR spectrum shows one resonance at δ -52.9 ppm assigned to the phosphane ligand PTA.

Solution studies

At variance with the poor solubility of the dichlorido adducts **1** and **2**, the organometallic derivatives **3**, **4-PF_6** and **5-Cl** are well soluble both in chlorinated and other polar organic solvents. The complexes were characterized in solution also by absorption UV-vis spectrophotometry. Spectra were recorded, in some cases, in various solvents (see Table S1 and Figures S1-S2 in the Supporting Information). The spectral profile of the ligand pbiH in the same solvents has been reported elsewhere.[14,15] The mononuclear platinum(II) complexes **2** and **3** and the heterodinuclear Pt^{II}/Au^{I} complexes **4-PF_6** and **5-Cl** exhibit, in DMSO, intense transitions in the range 342-345 nm which are assigned as LMCT bands characteristic of the Pt(II) chromophore. Additional bands in

the range 291-297 nm are attributed to a metal-perturbed intraligand (IL) π–π* transition within the pbi ligand. Besides these, additional bands between 261 and 276 nm are displayed in the spectra of compounds **4-PF$_6$** and **5-Cl**, assigned to the phosphane ligands at the gold(I) centres.

Prior to the biological assays, the solution chemistry of **3**, **4-PF$_6$** and **5-Cl** was analyzed under physiological-like conditions using UV-vis spectrophotometry. The compounds were first dissolved in DMSO and the resulting solutions (10^{-2} M) diluted in the reference phosphate buffer (PB), at pH 7.4, to final concentrations of $3x10^{-5}$ M (**3**) or 10^{-4} M (**4-PF$_6$** and **5-Cl**). Solutions were monitored over 24 h at room temperature (**3**) or 48 h at 37 °C (**4-PF$_6$** and **5-Cl**), and representative spectral profiles of **3**, **4-PF$_6$** and **5-Cl** are shown respectively in Figures S3, S4 and 2. Contrary to what observed in the case of the pbi-gold(I) mononuclear compounds, where the TPA ligand was found to confer extra stability to the complex,[14] in this case **5-Cl**, bearing the Au(TPA) unit, turned out to be the least stable. As shown in Figure 2, compound **5-Cl** is quite stable within two hours, while, after this period, the intensity of the absorption band at 338 nm began to decrease. At variance, the band at 232 nm showed a blue-shift and an increased intensity. After 10 hours, the spectral profile remained unchanged. Conversely, compound **4-PF$_6$** resulted stable for at least 19 hours, thereafter the intensity of the absorption band at 339 nm gradually decreased within 30 hours and then remained stable. In order to gain further insight into the solution behaviour of compounds **3** and **4-PF$_6$** in a coordinative solvent, ^{1}H NMR spectra were recorded in CD_3CN and monitored over 20 h at room temperature. The proton spectrum of **3** (data reported in the Experimental Section) remained unchanged while that of the cationic complex **4-PF$_6$** showed some changes in the aromatic region: *e.g.* broadening of the H^3 and H^4 signals. In the case of **4-PF$_6$** ^{31}P NMR spectra were also recorded over 20 h and also in this case was observed broadening of the PPh_3 signal. Such changes may be due to a fluxional behaviour of the $AuPPh_3$ fragment.

Finally, the stability of compounds **4-PF$_6$** and **5-Cl** towards reducing agents was evaluated (Figure 3). Sodium ascorbate (NaAsc) and reduced glutathione (GSH), one of the most important intracellular reducing agent, were chosen to mimic the biological milieu. Following the addition of 10:1 molar ratio of NaAsc, compound **4-PF$_6$** was not stable, the spectrum shows that the intensity of the absorption band at 338 nm decreased, probably due to a precipitation phenomenon. At variance, complex **5-Cl** was quite stable within 1 hour, then the intensity of the band at 336 nm gradually decreases within 5 hours and thereafter remained stable. A similar behaviour was observed, but more quickly for both compounds **4-PF$_6$** and **5-Cl**, following the addition of GSH: in both cases was observed a blue-shift of the main absorption band which suggests the formation of different species. However, reduction of the gold(I) center was never observed after the addition of these reducing agents.

Antiproliferative activity of study compounds

The antiproliferative effects of the study compounds were evaluated *in vitro* according to the procedures described by Skehan et al.,[24] and expressed as IC_{50} values (drug concentrations required to inhibit cell growth by 50%). All compounds were tested against the cisplatin-sensitive and cisplatin-resistant human ovarian cancer cell lines A2780/S and A2480/R, respectively; data are reported in Table 1.

While the free ligand showed a moderate cytotoxicity with IC_{50} values of 45.3 and 60.0 μM against the sensitive and the resistant cell lines, respectively, coordination of at least one metal centre typically resulted into greater cytotoxic effects. Of the two mononuclear adducts $[MCl_2(pbiH)]$, the palladium complex **1** showed a remarkable activity against both cell lines, showing IC_{50} values in the low micromolar range, thus being comparable to the gold(III) adduct $[Au(pbi)Cl_2]$,[14] while the activity of the platinum complex **2** was only moderate. Furthermore, compound **1** resulted more active against the cisplatin-resistant line (RI = 0.5), while **2** showed a positive RI value (1.7). At variance, the organometallic platinum(II) mononuclear compound **3** manifested a remarkable antiproliferative activity towards both the sensitive and the resistant A2780 cell lines, with IC_{50} values of 1.07 and 1.61 μM, respectively. Such a dramatic difference in the cytotoxic properties between platinum(II) coordination and organometallic derivatives of the same carrier ligand was previously observed, for example, in the case of $[PtCl_2(COD)]$ and [PtMeCl(COD)] (COD = 1,5-cyclooctadiene);[25] it seems to be a general rule not only for platinum(II)[26] but also for palladium(II) derivatives.[27] Most remarkably, the anchoring of the cytotoxic unit $Au(Ph_3P)$ to the Pt species resulted into a further marked increase of the antiproliferative effects. In fact, compound **4-PF$_6$** showed IC_{50} values of 0.19 and 0.37 μM towards A2780/S and A2780/R, respectively, even lower than those observed for the parent compounds **3** and $[Au(pbiH)(PPh_3)][PF_6]$.[14] Notably, the 1:1 combination of these two compounds showed similar activity to compound **4-PF$_6$** against both cell lines, with IC_{50} values of 0.2 and 0.51 μM in, respectively, A2780/S and A2780/R cells (*vs.* 0.19 and 0.37 μM for **4-PPF$_6$**). Thus, it seems that the two metallic species present in the heterodimetallic compounds do not manifest a synergistic effect but rather an additive effect. On the other hand, it is remarkable that joining the two metallic species in the same molecular scaffold does not reduce the biological action of each of them.

At variance with what observed for **4-PF$_6$**, the presence of the Au(TPA) moiety in compound **5-Cl** caused a significant decrease of the antiproliferative activity towards both cell lines. Surprisingly, the IC_{50} values reported for compound **5-Cl** are even higher than those observed for the parent compounds **3** and [Au(pbi)(TPA)],[14] and comparable to those of the free ligand.

Biomolecular Interactions: ESI MS studies

The interactions of the lead compounds **3** and **4-PF$_6$** with three selected model proteins - hen egg white lysozyme (lysozyme), bovine pancreatic ribonuclease (RNase A) and horse heart cytochrome c (cyt c) - and one oligonucleotide (ODN4: 5'-CGC GCG-3') were analysed through ESI-MS as the latter method appears to be highly suitable, direct and informative to monitor the binding behaviour of these biomolecules in solution. The resulting deconvoluted ESI-MS spectra are shown respectively in Figures S6, S7, 4 and 5. Lysozyme results not to interact with the two tested compounds; in contrast, formation of stable metal-protein adducts with cyt c and RNase A is clearly documented by the appearance of peaks of higher molecular mass than those of the native proteins. Remarkably, formation of adducts with cyt c and RNase A implies disruption of the starting metal complexes and/or loss of one or more ligands.

In the case of compound **3**, the predominant adduct with both proteins (cyt c and RNase A) is straightforwardly assigned to protein binding of [Pt(pbi)(Me)] fragments; however, a second intense peak, corresponding to a different stoichiometry – i.e. 2:1 Pt/protein – was observed with cyt c (Figure S6). Interestingly, compound **4-PF$_6$** interacts with RNase A in a different way; the ESI MS spectrum shows two peaks at 13878.22 Da and 14071.55 Da, which represent the adducts with bare Au(I) (Figure 4B). It seems that RNase A shows some kind of selectivity for gold over platinum, which is not shown by cytochrome c. Nevertheless, when the ODN4-**4PF$_6$** solutions were analyzed, (Fig. 5), new peaks corresponding to the metal fragments bound to one or two ODN4 molecules were detected. In particular, only one peak was found associated to [Pt(pbi)(Me)] fragment, while peaks corresponding to ODN4/AuPPh$_3$ or ODN4/Au(I) adducts were identified with different stoichiometry. This finding suggests that the complex may break down releasing bare Au(I) or AuPPh$_3$ species during adduct formation. With compound **3** the spectrum shows only one peak related to the ODN4/[Pt(pbi)(Me)] adduct (Figure S7).

The presence of different metal centers in the same molecule, as in **4-PF$_6$**, may grant the opportunity to obtain different biomolecular adducts which could lead to enhanced cytotoxic effects owing to the additive effect of coupled metals.

Biomolecular Interactions: X-ray crystallography

To gain deeper insight on how compounds **3** and **4-PF$_6$** might interact with proteins, we have grown crystals of the adducts that they form with RNase A and solved the X-ray structures of both RNase A/**3** and RNase A/**4-PF$_6$** complexes. Monoclinic RNase A crystals with two molecules in the asymmetric unit were prepared following a procedure previously described[28] (see Experimental section for further details). To prepare the crystals of the adducts, native RNase A

crystals were soaked in solutions containing 2.5-5 mM of the compound. The structures of the resulting RNase A/**3** and RNase A/**4-PF$_6$** crystals were refined to R-factor of 0.195 and 0.183 (Rfree of 0.254 and 0.234) at 1.98 and 1.68 Å resolution, respectively. Crystallographic data and refinement statistics are listed in Table S2 in the Supporting information. The metal binding sites were determined by a comparative inspection of 2Fo-Fc (Figure 6A-C), Fo-Fc and anomalous difference Fourier (Figure 6D-F) electron density maps. The root mean square deviations of the carbon alpha atoms of molecules A and B in the adducts from those of the same molecules in the free RNase A structures (PDB code 1JVT) are within the range 0.34-1.33 Å (0.34-0.55 Å excluding residues 16-22 of molecule A in RNase A/**4-PF$_6$,** which adopt a different conformation), indicating that the overall structure of RNase A is preserved upon the binding of the two metal compounds. Analysis of the crystal structures of RNase A/**3** and RNase A/**4-PF$_6$** indicates that in both cases the binding occurs only in molecule A (Figure S8). This is not surprising; since it was already shown that accessibility of protein active site in molecule A of monoclinic crystals of RNase A is higher than that of molecule B.[29]

RNase A/**3** has two Pt binding sites located on the surface of the protein: close to His105 side chain and to His119 side chain, *i.e.* in the protein active site (Figure 6 A-B and C-D). The Pt center coordinates to NE2 atom of His105 and ND1 atom of His119 with unrestrained bond length of about 2.3 Å and occupancy value of 0.5 and 0.4, respectively. At variance, inspection of the electron density maps reveals that RNase A/**4-PF$_6$** presents a single metal binding site, close to His105 side chain (Figure 6 E-F). On the basis of mass spectrometry data collected on the RNase A/**4-PF$_6$** system, it could be inferred that a Au atom is bound to this site, although with low occupancy (occupancy value = 0.3). The Au coordinates to NE2 atom of His105 with bond length of 2.2 Å. Unfortunately in both structures, close to metal binding sites the electron density map is too poor to allow the modelling of metal ligands.

The finding that, under the same experimental conditions, a Pt containing fragment from **3** is able to bind the catalytically important residue His119 of RNase A whereas no fragments from **4-PF$_6$** are observed in the protein active site of the RNase A/**4-PF$_6$** adduct, prompted us to perform in solution catalytic activity studies of the enzyme in the absence and in the presence of the two compounds, separately. The catalytic activity of RNase A, free and in the presence of **3** and **4-PF$_6$**, on yeast RNA was evaluated by Kunitz method (see Experimental Section for further details). The presence of **4-PF$_6$** does not alter the catalytic activity of the protein, even at high metal compound to protein ratio (Figure S9). On the contrary, when the protein is incubated in the presence of **3**, a slight decrease in the catalytic power of the protein was observed, in particular at high metal compound to protein ratio (Figure S9). These data are in full agreement with crystallographic

results indicating that a fraction of molecules of RNase A/**3** adduct is characterized by an occluded active site cleft.

Experimental section

General remarks

All the solvents were purified and dried according to standard procedures. The ligand 2-(2-pyridyl)benzimidazole (pbiH) was synthesized by condensation reaction of pyridine-2-carboxylic acid with 1,2-phenylenediamine in the presence of polyphosphoric acid at 180 °C, according to a literature method.[21] *cis*-$[Pt(Me)_2(DMSO)_2]$ was synthesized according to ref. 22. Complex **1** was obtained as described in ref. 18. Elemental analyses were performed with a Perkin-Elmer elemental analyser 240B. ^1H and $^{31}P\{^1H\}$ NMR spectra were recorded with Varian VXR 300 and Bruker Avance III 400 spectrometers at 298 K. Chemical shifts are given in ppm relative to internal TMS for ^1H and external 85% H_3PO_4 for ^{31}P; *J* values are given in Hz. ^1H–^1H COSY and ^1H–^1H NOESY experiments were performed by means of standard pulse sequences. UV-vis spectra were recorded on a Varian Cary 50 or on a Hitachi U-2010 UV-vis spectrophotometer.

Spectroscopic data of 2-(2-pyridyl)benzimidazole (pbiH). Selected IR bands (ν_{max}/cm^{-1}): 3060 ν(N-H), 1593, 1568, 1400, 1314, 1280, 744, 703. ^1H NMR (300 MHz, $CDCl_3$): δ 10.77 (broad s, 1H; NH), 8.64 (dd, 1H, $J_{H\text{-}H}$ = 4.8, 1.7 Hz; H^6), 8.44 (dt, 1H, $J_{H\text{-}H}$ = 7.9, 1.1 Hz; H^3), 7.88 (td, 1H, $J_{H\text{-}H}$ = 8.4, 1.7, Hz; H^4), 7.86 (m, 1H, $J_{H\text{-}H}$ = 9.1, 1.6, 1.3 Hz; $H^{6'}$), 7.49 (m, 1H, $J_{H\text{-}H}$ = 9.3, 5.6, 1.9 Hz; $H^{3'}$), 7.38 (ddd, 1H, $J_{H\text{-}H}$ = 7.5, 4.8, 1.2 Hz; H^5), δ 7.30 (m, 2H, $J_{H\text{-}H}$ = 9.3, 6.7, 5.4, 1.2, 0.8 Hz; $H^{4'}$, $H^{5'}$). ^1H NMR (300 MHz, acetone-d_6): δ 12.11 (broad s, 1H; NH), 8.67 (d, 1H, $J_{H\text{-}H}$ = 4.8 Hz; H^6), 8.40 (d, 1H, $J_{H\text{-}H}$ = 7.8 Hz; H^3), 7.98 (td, 1H, $J_{H\text{-}H}$ = 8.0, 1.7 Hz; H^4), 7.69 (broad m, 2H, $J_{H\text{-}H}$ = 5.4 Hz; $H^{3'}$, $H^{6'}$), 7.47 (ddd, 1H, $J_{H\text{-}H}$ = 7.5, 4.8, 1.2 Hz; H^5), 7.26 (broad m, 2H; $H^{4'}$, $H^{5'}$). ^1H NMR (300 Mz, DMSO-d_6): δ 13.09 (broad s, 1H; NH), 8.72 (d, 1H, $J_{H\text{-}H}$ = 4.7 Hz; H^6), 8.31 (d, 1H, $J_{H\text{-}H}$ = 7.9 Hz; H^3), 7.99 (td, 1H, $J_{H\text{-}H}$ = 7.8, 1.7 Hz; H^4), 7.69 (m, 1H, $J_{H\text{-}H}$ = 9.3, 7.0, 2.1 Hz; $H^{6'}$), 7.51 (m, 2H; H^5+$H^{3'}$), 7.21 (m, 2H, $J_{H\text{-}H}$ = 7.4, 1.5 Hz; $H^{4'}$, $H^{5'}$).

$[PdCl_2(pbiH)]$ (1): An ethanol solution (10 mL) of pbiH (150 mg, 0.77 mmol) was added to a solution of K_2PdCl_4 (250 mg, 0.77 mmol) in the same solvent (30 mL). The resulting mixture was stirred in the dark for 6 h at 78 °C. The solid which formed was filtered off, washed with water, EtOH and Et_2O and dried under vacuum. Yield 87%. Mp > 400 °C. Anal. Calc. for $C_{12}H_9N_3Cl_2Pd$: C, 38.69; H, 2.43; N, 11.28%. Found: C, 38.39; H, 2.50; N, 11.09%. Selected IR bands (ν_{max}/cm^{-1}, Nujol): 1612, 1588, 1567, 1481, 1459, 1446, 341 and 324 ν(Pd-Cl);. ^1H NMR (300 MHz, DMSO-

d$_6$): δ 14.86 (broad s, 1H; NH), 9.09 (d, 1H, $J_{H\text{-}H}$ = 5.6 Hz; H^6), 8.68 (d, 1H, $J_{H\text{-}H}$ = 8.1 Hz; H^3), 8.40 (td, 1H, $J_{H\text{-}H}$ = 7.8, 1.6 Hz; H^4), 8.32 (d, 1H, $J_{H\text{-}H}$ = 7.0 Hz; $H^{6'}$), 7.81 (ddd, 1H, $J_{H\text{-}H}$ = 7.4, 5.7, 1.6 Hz; H^5), 7.76 (d, 1H, $J_{H\text{-}H}$ = 8.3 Hz; $H^{3'}$), 7.48 (td, 1H, $J_{H\text{-}H}$ = 7.0, 1.3 Hz; $H^{5'}$), 7.40 (td, 1H, $J_{H\text{-}H}$ = 8.4, 1.3 Hz; $H^{4'}$).

[PtCl$_2$(pbiH)] (2): A dichloromethane solution (10 mL) of pbiH (97.6 mg, 0.5 mmol) was added to a solution of *cis*-[PtCl$_2$(DMSO)$_2$] (211 mg, 0.5 mmol) in the same solvent (30 mL). The mixture was stirred in the dark for 3h at room temperature. The yellow solid which formed was filtered off and dried under vacuum. Yield 81%. Mp 239 °C (dec.). Anal. Calc. for $C_{12}H_9N_3Cl_2Pt$: C, 31.25; H, 1.97; N, 9.11%. Found: C, 31.19; H, 1.85; N, 9.02%. Selected IR bands (ν_{max}/cm^{-1}, Nujol): 1614, 1590, 1496, 1483, 344 and 328 ν(Pt-Cl); ^{1}H NMR (300 MHz, DMSO-*d*$_6$): δ 13.53 (broad s, 1H; NH), 9.46 (d, 1H, $J_{H\text{-}H}$ = 5.7 Hz; H^6), 8.78 (d, 1H, $J_{H\text{-}H}$ = 8.4 Hz; H^3), 8.44 (t, 1H, $J_{H\text{-}H}$ = 7.8 Hz; H^4), 8.31 (d, 1H, $J_{H\text{-}H}$ = 7.8 Hz; $H^{6'}$), 7.83-7.78 (m, 2H; $H^{3'}$+ H^5), 7.51 (pseudo t, 1H, $J_{H\text{-}H}$ = 7.5, 7.2 Hz; $H^{5'}$), 7.42 (pseudo t, 1H, $J_{H\text{-}H}$ = 8.1, 7.2 Hz; $H^{4'}$).

[Pt(pbi)(Me)(DMSO)] (3): A dichloromethane solution (10 mL) of pbiH (97.6 mg, 0.5 mmol) was added to a solution of *cis*-[PtMe$_2$(DMSO)$_2$] (190.7 mg, 0.5 mmol) in the same solvent (30 mL). The mixture was stirred in the dark for 24 h at room temperature. Afterward the solution was filtered and concentrated to a small volume; addition of diethyl ether afforded a yellow solid that was filtered off and vacuum dried to give the analytical sample. Yield 72%. Mp 393 °C. Anal. Calcd for $C_{15}H_{18}N_3OPtS$: C, 37.34; H, 3.55, N, 8.71%. Found: C, 37.10; H, 3.55; N, 8.82%. Selected IR bands (ν_{max}/cm^{-1}, Nujol): 1613, 1567, 1167, 1117, 888, 740. ^{1}H NMR (400 MHz, CD_2Cl_2): δ 9.50 (d, 1H, $J_{H\text{-}H}$ = 6.0, $^3J_{Pt\text{-}H}$ = 21.2 Hz; H^6), 8.24 (d, 1H, $J_{H\text{-}H}$ = 7.6 Hz; H^3), 7.89 (t, 1H, $J_{H\text{-}H}$ = 7.6 Hz; H^4), 7.77 (d, 1H, $J_{H\text{-}H}$ = 8.0 Hz; $H^{3'}$), 7.61 (d, 1H, $J_{H\text{-}H}$ = 7.6 Hz; $H^{6'}$), 7.30 (t, broad, 1H, $J_{H\text{-}H}$ = 6.8 Hz; H^5), 7.05 (m, 2H, $J_{H\text{-}H}$ = 7.6 Hz, $H^{4'}$, $H^{5'}$), 3.34 (s, 6H, $^3J_{Pt\text{-}H}$ = 32.4 Hz; Me-DMSO), 1.16 (s, 3H, $^2J_{Pt\text{-}H}$ = 78.8 Hz; Me). ^{1}H NMR (400 MHz, CD_3CN): δ 9.60 (d, 1H, $J_{H\text{-}H}$ = 5.2, $^3J_{Pt\text{-}H}$ = 20.4 Hz; H^6), 8.28 (d, 1H, $J_{H\text{-}H}$ = 7.6 Hz; H^3), 8.07 (td, 1H, $J_{H\text{-}H}$ = 8.0, 1.6 Hz; H^4), 7.85 (dd, 1H, $J_{H\text{-}H}$ = 7.2, 2.4 Hz; $H^{3'}$), 7.65 (dd, 1H, $J_{H\text{-}H}$ = 6.0, 2.0 Hz; $H^{6'}$), 7.49 (ddd, 1H, $J_{H\text{-}H}$ = 7.6, 6.0, 1.6 Hz; H^5), 7.12 (m, 2H, $J_{H\text{-}H}$ = 7.2, 1.6 Hz, $H^{4'}$, $H^{5'}$), 3.41 (s, 6H, $^3J_{Pt\text{-}H}$ = 32.8 Hz; Me-DMSO), 1.23 (s, 3H, $^2J_{Pt\text{-}H}$ = 80.4 Hz; Me). Assignments based on 2D-COSY and NOESYspectra.

[(PPh$_3$)Au(μ-pbi)Pt(Me)(DMSO)][PF$_6$] (4-PF$_6$): A solution of [AuCl(PPh$_3$)] (241.7 mg, 0.5 mmol) and $AgPF_6$ (126.4 mg, 0.5 mmol) in dichloromethane (30 mL) was stirred in the dark until AgCl precipitation was completed. Then, the filtered solution was added to a solution of **3** (241.7 mg, 0.5 mmol) in the same solvent (20 mL). The mixture was stirred in the dark for 4h at room temperature. Afterward the solution was filtered and concentrated to a small volume; addition of diethyl ether gave a yellow solid which was filtered off and vacuum dried to give the analytical

sample. Yield 71%. Mp: 163 °C (dec.). Anal. Calcd for $C_{33}H_{32}AuF_6N_3OP_2PtS$: C, 36.47; H, 2.97; N, 3.87%. Found: C, 36.19; H, 3.01; N, 3.68 %. Selected IR bands (ν_{max}/cm^{-1}, Nujol): 1609, 1019 (PPh_3), 840 (PF_6), 748, 712. ^{1}H NMR (400 MHz, $CDCl_3$): δ 9.64 (d, 1H, J_{H-H} = 5.6, Hz; H^6), 8.82 (broad d, 1H; H^3), 7.95 (t, 1H, J_{H-H} = 8.0 Hz; H^4), 7.89 (d, 1H, J_{H-H} = 8.0 Hz; $H^{3'}$), 7.75 (d, 1H, J_{H-H} = 8.0 Hz; $H^{6'}$), 7.56-7.40 (m, 16H; H^5 +H-PPh_3), 7.26 (t, 2H, J_{H-H} = 7.6 Hz, $H^{4'}/H^{5'}$), 7.19 (t, J_{H-H} = 7.8 Hz, $H^{5'}/H^{4'}$), 3.42 (s, 6H, $^3J_{Pt-H}$ 30.4 Hz; Me-DMSO), 1.20 (s, 3H, $^2J_{Pt-H}$ = 73.2 Hz; Me). ^{1}H NMR (400 MHz, CD_3CN): δ 9.70 (d, 1H, J_{H-H} = 5.6, Hz; H^6), 8.86 (broad d, 1H; H^3), 7.99 (t, 1H, J_{H-H} = 8.0 Hz; H^4), 7.91 (d, 1H, J_{H-H} = 8.0 Hz; $H^{3'}$), 7.84 (broad d, 1H, J_{H-H} = 6.8 Hz; $H^{6'}$), 7.81 (dt, 1H, J_{H-H} = 8.0, 1.6 Hz; H^5) 7.70-7.63 (m, 15H; H-PPh_3), 7.23 (m, 2H, J_{H-H} = 8.0, 6.8 Hz, $H^{4'}$, $H^{5'}$), 3.40 (s, 6H, $^3J_{Pt-H}$ 34.4 Hz; Me-DMSO), 1.12 (s, 3H, $^2J_{Pt-H}$ = 78.4 Hz; Me). ^{31}P NMR (161.9 MHz, $CDCl_3$): δ 33.2 (s, PPh_3); -144.1 (hept, PF_6). ^{31}P NMR (161.9 MHz, CD_3CN): δ 30.9 (s, PPh_3); -144.6 (hept, PF_6).

[(TPA)Au(μ-pbi)Pt(Me)(DMSO)]Cl (5-Cl): An acetone solution (20 mL) of [Pt(pbi)(Me)(DMSO)] (154.6 mg, 0.32 mmol) was added a suspension of [Au(TPA)Cl] (125.2 mg, 0.32 mmol) in the same solvent (30 mL). The mixture was stirred for 24 h at room temperature in the dark. Afterward the solution was filtered and concentrated to a small volume; addition of diethyl ether afforded a beige solid that was filtered off and vacuum dried to give the analytical sample. Yield 57%. Mp: 165 °C. Anal. Calcd for $C_{21}H_{29}AuClN_6OPPtS$: C, 28.92; H, 3.35; N, 9.64%. Found: C, 29.02; H, 3.14; N, 9.55%. Selected IR bands (ν_{max}/cm^{-1}, Nujol): 1609, 1279, 1151, 1098, 1014, 948, 741. ^{1}H NMR (400 MHz, acetone-d_6): 9.67 (d, 1H, J_{H-H}= 6.0, $^3J_{Pt-H}$ = 19.2 Hz; H^6), 8.33 (d, 1H, J_{H-H} = 7.6 Hz, H^3), 8.17 (t, 1H, J_{H-H} = 8.0, 7.2 Hz, H^4), 7.83 (dd, 1H, J_{H-H} = 7.2, 1.6 Hz, $H^{3'}$), 7.64 (dd, 1H, J_{H-H} = 6.0, 2.4 Hz, $H^{6'}$), 7.56 (t, 1H, J_{H-H} = 6.0, Hz, H^5), 7.08 (m, 2H, $H^{4'}$, $H^{5'}$), 4.68 (d, 3H, J_{AB} = 12.4 Hz, 3 N-C$H_A$$H_B$-N), 4.56 (d, 3H, J_{AB} = 12.4 Hz, 3 N-C$H_A$$H_B$-N), 4.45 (s, 6H, 3 N-$CH_2$-P), 3.54 (s, 6H, $^3J_{Pt-H}$ = 32.8 Hz, CH_3-DMSO), 1.26 (s, 3H, $^2J_{Pt-H}$ = 79.2 Hz, CH_3). ^{31}P NMR (161.9 MHz, acetone-d_6): δ -52.9 (s, TPA).

UV-visible spectrophotometric studies

The electronic spectra were recorded diluting small amounts of freshly prepared concentrated solutions of the individual complexes in DMSO in phosphate buffer pH 7.4 or in ammonium acetate pH 6.8 (spectral profiles shown in Figure S5). The concentration of each compound in the final sample was 10^{-4} M or 3 x 10^{-5} M.

Sample preparation and mass spectrometric analysis

Metal complex/protein samples were prepared by mixing, in 20 mM ammonium acetate buffer pH 6.8, protein (i.e. cyt c, Lysozyme, RNase A) at 100 μM concentration and the metal complex in 3:1 metal/protein ratio. The solution was incubated at 37°C for 24h; after this time, water was added to the mixture up to 5 μM final concentration.

Metal complex/ODN4 adducts were prepared by mixing equivalent amounts of the ODN4 (50 μM) and complexes in water at 37 °C. After 24h incubation, CH_3OH was added to the reaction mixture before the analysis, carried out at final concentration of 25 μM (50% CH_3OH).

ESI-MS spectra were recorded by direct introduction at 5 μl/min flow rate in an Orbitrap high-resolution mass spectrometer (Thermo, San Jose, CA, USA), equipped with a conventional ESI source. The working conditions were the following: spray voltage 3.1 kV, capillary voltage 45 V and capillary temperature 220°C. The sheath and the auxiliary gases were set, respectively, at 17 (arbitrary units) and 1 (arbitrary units). For acquisition, Xcalibur 2.0. software (Thermo) was used and monoisotopic and average deconvoluted masses were obtained by using the integrated Xtract tool. For spectrum acquisition a nominal resolution (at m/z 400) of 100,000 was used.

Preparation of crystals, X-ray diffraction data collection, refinement and X-ray structural analysis of RNase A/3 and RNase A/4-PF_6

RNase A crystals were obtained using the procedure previously described by Vitagliano *et al.,* 2000[28]. Briefly, crystals of the protein were grown by hanging drop vapor diffusion method using a reservoir solution containing 22-24 % (w/v) PEG4K, 10 mM sodium citrate pH 5.1-5.3. The crystals are monoclinic, space group C2, with two molecules in the asymmetric unit. The adducts were prepared by a three-days soaking in a solution that comprised the standard mother liquor used for the crystal growth to which a 2.5-5 mM solution of each compound was added. Crystal soaked in this solution were mounted for the X-ray data collection without using a cryoprotectant, as done in previous studies[30].

X-ray diffraction data were collected at 100 K using a Saturn944 CCD detector equipped with CuKα X-ray radiation from a Rigaku Micromax 007 HF generator at the CNR Institute of Biostructures and Bioimages, Napoli, Italy. Data were processed, scaled and merged using HKL2000[31]. Data collection statistics are reported in Table S2.

The structures were solved by molecular replacement method, using the molecule A of PDB file 1JVT[29], without water molecules, as starting model. The refinement was carried out with Refmac5.7[32], model building and map inspections were performed using Coot [33]. 5% of the data was used for calculation of the R-free value. After several rounds of refinement using the maximum

likelihood option in Refmac, manual adjustments of side-chain atoms and addition of metals, water molecules and other ligands (acetate and sulfate ions) to the coordinates, the structures converged to Rfactor of 0.191 and 0.183 (Rfree of 0.253 and 0.234), for RNase A/**3** and RNase A/**4-PF$_6$**, respectively. Refinement statistics are reported in Table S2. Structure validation has been carried out using Procheck[34]. Coordinates and structure factors were deposited in the Protein Data Bank under the accession codes 5E5E and 5E5F for RNase A/3 and RNase A/4-PF6, respectively.

RNase catalytic assay

The catalytic activity of RNase A and of the adducts formed in the reaction of the protein with **3** and **4-PF$_6$** towards yeast RNA was determined by the Kunitz spectrophotometric assay[35], as previously done in other works[36], using 0.5 mg x mL^{-1} of RNA in 50 mM sodium acetate/acetic acid buffer, pH 5.0, at 298 K. Spectrophotometric measurements were performed with a Jasco spectrophotometer. Enzyme concentration was 0.1 μg x mL^{-1}. Experiments were repeated three times and performed after 24 h of incubation, with protein to metal ratio 1:2, 1:5, 1:10.

Conclusions

A novel organometallic platinum(II) complex **(3)** bearing the pbi ligand has been synthesised and characterised showing remarkable antiproliferative properties and the ability to overcome cisplatin resistance. This complex may be straightforwardly transformed into the corresponding heterobimetallic gold-platinum complexes by reaction with gold phosphanes: two distinct heterobimetallic complexes were specifically prepared either with AuPPh$_3$ and AuPTA as attached metallic fragments to the organometallic Pt(II) complex.

The new heterobimetallic complexes were extensively characterised by NMR and UV-vis manifesting acceptable stability and solubility profiles in aqueous environments; these features render them well amenable for standard *in vitro* pharmacological testing.

Notably, the organometallic complex **3** demonstrated far enhanced cytotoxic properties when compared to the corresponding platinum(II) coordination compound **2**; in addition it is able to overcome completely cisplatin resistance. It is inferred that the CH$_3$-Pt motif is a key feature for the biological profile. Afterward, the antiproliferative properties of the two heterobimetallic complexes were also assayed in comparison to the parent mononuclear platinum(II) and gold(I) compounds in a representative cancer cell lines *i.e.* A2780S/R. Interestingly, the heterobimetallic Pt-Au complex bearing the triphenylphosphine ligand manifested highly enhanced cytotoxic effects compared to mononuclear Pt complex **3**. An additive rather than a synergistic effect of the two different metal

centres is suggested by the comparable inhibitory effects displayed by a combination of the parent platinum(II) and gold(I) compounds and the Pt-Au complex. On the other hand, it is remarkable that joining the two metallic species in the same molecular scaffold does not reduce the biological action of each of them.

To gain some deeper insight into the underlying mechanisms and interactions, we analysed the reactivity of the study compounds with a few representative biomolecular targets i.e. cyt c, Lysozyme, RNase A and ODN4 by ESI-MS and X-ray crystallography. ESI-MS revealed that a number of adducts are indeed formed with the model proteins cyt c and RNase A and with the standard oligonucleotide ODN4 and their nature could be identified. Furthermore mass spectrometry data suggest that **4-PF$_6$** presents a different behaviour when reacted with proteins compared to its monometallic counterpart **3**. In addition, X-ray structures of the adducts formed in the reaction between RNase A and both **3** and **4-PF$_6$** were solved. Crystal structures point out that bare Pt and Au ions are bound to His residues in RNase A catalytic region. Thus joint analysis of the ESI-MS and crystallographic data of the protein adducts allows us to state that this Au-Pt heterodimetallic compound undergoes transformation and cleavage upon protein binding so that only monometallic fragments are found associated to biomolecules. His residues appear to be the major binding site for both Pt and Au metal ions derived from the starting compound.

To the best of our knowledge, our study offers the second example in the literature for heterodimetallic Pt(II)-Au(I) complexes showing remarkable cytotoxic properties,[13] and the first featuring an organoplatinum(II) moiety. In addition, the detailed structural characterization of an adduct formed in the reaction between a protein and a heterodimetallic compound is provided with relevant mechanistic implications.

Acknowledgments

Luigi Messori and Lara Massai gratefully acknowledge Beneficentia Stiftung (Vaduz, Liechtenstein), AIRC (IG- 16089) and COST Action CM1105 for generous financial support and Prof. Carla Bazzicalupi for the gift of ODN4. M.A.C. gratefully acknowledges the Regione Autonoma della Sardegna (RAS) for the grant “Premialità Regionale 2011”. G.F and A.M. thank M. Amendola and G. Sorrentino for technical assistance in the X-ray diffraction data collection. We thank Dr. Elena Michelucci for recording ESI-MS spectra at CISM.

Notes and References

[1] (a) Martindale: *The complete drug reference*, ed. S. C. Sweetma,n, Pharmaceutical Press, London, 35th edn, 2007; (b) M. Watson, A. Barrett, R. Spence and C. Twelves, *Oncology*, Oxford University Press, Oxford, 2nd edn, 2006.

[2] (a) C. A. Rabik and M. E. Dolan, *Cancer Treat. Rev*., 2007, **33**, 9-23; (b) L. Kelland, *Nat. Rev. Cancer*, 2007, **7**, 573-584.

[3] (a) C. X. Zhang and S. J. Lippard, *Curr. Opin. Chem. Biol*., 2003, **7**, 481-489; (b) N. J. Wheate, S. Walker, G. E. Craig and R. Oun, *Dalton Trans*., 2010, **39**, 8113-8127.

[4] (a) N. P. Barry, P. J. Sadler, *Chem. Commun*., 2013, **49**, 5106-5131; (b) N. Muhammad and Z. Guo, *Curr. Opin. Chem. Biol.,* 2014, **19**, 144-153.

[5] (a) M. D. Hall, H. R. Mellor, R. Callaghan and T. W. Hambley, *J. Med. Chem*., 2007, **50**, 3403–3411; (b) E. Reisner, V. B. Arion, B. K. Keppler and A. J. L. Pombeiro, *Inorg. Chim. Acta*, 2008, **361**, 1569–1583.

[6] M. Coluccia and G. Natile, *Anti-Cancer Agents Med. Chem*., 2007, **7**, 111-123.

[7] T. C. Johnstone, J. J. Wilson and S. J. Lippard, *Inorg. Chem*., 2013, **52**, 12234-12249.

[8] N. J. Wheate and J. G. Collins, *Coord. Chem. Rev*., 2003, **241**, 133-145.

[9] (a) P. C. A. Bruijnincx and P. J. Sadler, *Curr. Opin. Chem. Biol*., 2008, **12**, 197-206; (b) K. S. Lovejoy and S. J. Lippard, *Dalton Trans*., 2009, 10651-10659.

[10] (a) M. J. Clarke, *Coord. Chem Rev*., 2003, **236**, 209-233; (b) G. Suss-Fink, *Dalton Trans*., 2010, **39**, 1673-1688; (c) G. Sava, A. Bergamo and P. J. Dyson, *Dalton Trans*., 2011, **40**, 9069-9075; (d) W.H. Ang, A. Casini, G. Sava and P. J. Dyson, *J. Organomet. Chem*., 2011, **696**, 989-998.

[11] (a) S. J. Berners-Price and A. Filipovska, *Metallomics*, 2011, **3**, 863-873; (b) L. Ronconi and D. Fregona, *Dalton Trans*., 2009, 10670-10680; (c) C.-M. Che and R. W.-Y. Sun, *Chem. Commun*., 2011, **47**, 9554-9560; (d) B. Bertrand and A. Casini, *Dalton Trans*., 2014, **43**, 4209-4219.

[12] For Pt/Ru complexes see for instance: (a) A. Herman, J. M. Tanski, M. F. Tibbetts and C. M. Anderson, *Inorg. Chem.*, 2007, **47**, 274–280; (b) C. M. Anderson, I. R. Taylor, M. F. Tibbetts, J. Philpott, Y. Hu and J. M. Tanski, *Inorg. Chem*., 2012, **51**, 12917–12924.

[13] For Pt/Au complexes see for instance: M. Wenzel, E. Bigaeva, P. Richard, P. Le Gendre, M. Picquet, A. Casini, E. Bodio, *J. Inorg. Biochem*., 2014, **141**, 10-16.

[14] M. Serratrice, M. A. Cinellu, L. Maiore, M. I. Pilo, A. Zucca, C. Gabbiani, A. Guerri, I. Landini, S. Nobili, E. Mini, L. Messori, *Inorg. Chem.*, 2012, **51**, 3161-3171.

[15] L. Maiore, M. C. Aragoni, C. Deiana, M. A. Cinellu, F. Isaia, V. Lippolis, A. Pintus, M. Serratrice, M. Arca, *Inorg. Chem.*, 2014, **53**, 4068-4080.

[16] (a) C. Mock, I. Puscasu, M.J. Rauterkus, G. Tallen, J.E.A. Wolff and B. Krebs, *Inorg. Chim. Acta*, 2001, **319**, 109-106; (b) G. Tallen, C. Mock, S.B. Gangopadhyay, B. Kangarloo, B. Krebs and

J.E.A. Wolff, *Anticancer Res*., 2000, **20**, 445.

[17] F. Gümüs, I. Pamuk, T. Özden, S. Yildiz, N. Diril, E. Öksüzoglu, S. Gür and A. Özkul, *J. Inorg. Biochem*., 2003, **94**, 255-262.

[18] J. S. Casas, A. Castineiras, E. Garìa-Martinez, Y. Parajò, M. L. Pérez-Parallé, A. Sànchez-Gonzàlez, and J. Sordo, *Z. Anorg. Allg. Chem*., 2005, 2258-2264.

[19] X. Wang and Z. Guo in: *Bioinorganic Medicinal Chemistry*, E. Alessio (Ed.), WILEY-VCH Verlag GmbH & Co. KGaA, Weinheim, 2011, pp 97-149.

[20] (a) G. Gasser, I. Ott, and N. Metzler-Nolte, *J. Med. Chem*., 2011, **54**, 3-25; (b) A. L. Noffke, A. Habtemariam, A. M. Pizarro and P. J. Sadler, *Chem. Commun*., 2012, **48**, 5219-5246; (c) C. G. Hartinger, N. Metzler-Nolte and P. J. Dyson, *Organometallics*, 2012, **31**, 5677-5685.

[21] Alcade, E.; Dinarés, I.; Pérez-Garcìa, L.; Roca, T. *Synthesis*, 1992, **4**, 395-397.

[22] Eaborn, C.; Kundu, K.; Pidcock, A., *J. Chem. Soc., Dalton Trans*., 1981, 933-938.

[23] Tipically, PPh_3 bound to platinum(II) *trans* to a pyridine nitrogen resonates at *ca.* 24 ppm, with $J_{Pt\text{-}P}$ of *ca.* 4300 Hz. See, for example, A. Zucca, G.L. Petretto, S. Stoccoro, M.A. Cinellu, M. Manassero, C. Manassero and G. Minghetti, *Organometallics*, 2009, **28**, 2150-2159

[24] P.Skehan, R.Storeng, D. Scudiero, A. Monks, J. McMahon, D. Vistica, J. T. Warren, H. Bokesch, S. Kenney, M. R. Boyd, *J. Natl Cancer Inst*., 1990, **82**, 1107–1112.

[25] K. Butsch, S. Elmas, N. Sen Gupta, R. Gust, F. Heinrich, A. Klein, Y. von Mering, M. Neugebauer, I. Ott, M. Schäfer, H. Scherer and T. Schurr, *Organometallics*, 2009, **28**, 3906.

[26] A. Lüning, J. Schur, L. Hamel, I. Ott and A. Klein, *Organometallics,* 2013, **32**, 3662-3672; and references therein.

[27] C. Cullinane, G. B. Deacon, P. R. Drago, T. W. Hambley, K. T. Nelson and L. K. J. Webster, *Inorg. Biochem*., 2002, **89**, 293.

[28] L.Vitagliano, A. Merlino, A. Zagari, L. Mazzarella. *Protein Science* 2000, **9**, 1217-1225.

[29] L.Vitagliano, A. Merlino, A. Zagari, L. Mazzarella. *Proteins :Structure, Function, and Genetics* 2002, **46**, 97-104.

[30] I. Russo Krauss, L. Messori, M. A. Cinellu, D. Marasco, R. Sirignano, A. Merlino. *Dalton Trans* 2014, **43(46),** 17483-8.

[31] Z. Otwinowski, W. Minor. *Methods Enzymol* 1997, **276**, 307.

[32] N.Murshudov, P. Skubak, A.A. Lebedev, N.S. Pannu, R.A. Steiner, R.A. Nicholls, M.D. Winn, F. Long, A.A. Vagin. *Acta Cryst D* 2011, **67**, 355.

[33] P. Emsley, K. Cowtan. *Acta Cryst D* 2004, **60**, 2126.

[34] R.A. Laskowski, M.W. Macarthur, D.S. Moss, J.M. Thornton. *J Appl Cryst* 1993, **26**, 283.

[35] M. Kunitz, *J. Biol. Chem*. 1946, **164**, 563.

[36] (a) L. Messori, F. Scaletti, L. Massai, M. A. Cinellu, I. Russo Krauss, G. di Martino, A. Vergara, L. Paduano, A. Merlino. *Metallomics*. 2014, **6**, 233; (b) D. Picone, F. Donnarumma, G. Ferraro, I. Russo Krauss, A. Fagagnini, G. Gotte, A. Merlino *J Inorg Biochem*. 2015, **146**, 37.

Schemes and Figures

Table 1. Drug sensitivity profiles of cisplatin-sensitive and -resistant human ovarian carcinoma cell lines (A2780/S and A2780/R) towards the study compounds. For comparison purposes the values obtained with cisplatin are reported.

	IC_{50} (μM) ± SD		
Compounds	**A2780/S**	**A2780/R**	**RI**
pbiH	45.30 ± 1.40	60.00± 3.40	1.3
$[Au(pbi)Cl_2]$[a]	6.60 ± 4.01	5.31 ± 0.66	0.8
$[PdCl_2(pbiH)]$ **(1)**	4.01 ± 0.91	1.86 ± 0.62	0.5
$[PtCl_2(pbiH)]$ **(2)**	22.51±4.37	38.01 ± 6.95	1.7
[Pt(pbi)(Me)(DMSO)] **(3)**	1.07 ± 0.13	1.61 ± 0.48	1.5
$[(PPh_3)Au(\mu\text{-pbi})Pt((Me)(DMSO)][PF_6]$ **(4-PPF$_6$)**	0.19 ± 0.03	0.37 ± 0.05	2
$[Au(pbiH)(PPh_3)][PF_6]$[a]	1.50 ± 0.10	2.00 ± 0.10	1.3
$[Au(pbi)(PPh_3)]$[a]	0.60 ± 0.05	0.90 ± 0.02	1.5
[(TPA)Au(μ-pbi)Pt(Me)(DMSO)]Cl **(5-Cl)**	35.24 ± 9.42	>50	-
[Au(pbi)(TPA)][a]	13.30 ± 2.61	28.83 ± 1.04	1.2
3 + $[Au(pbiH)(PPh_3)][PF_6]$	0,20 ± 0.08	0,51 ± 0.06	2.53
CDDP	1.81 ± 0.68	27.54 ± 5.02	15.2

Results are the mean of at least three independent experiments; SD, standard deviation; RI, resistance index. [a]Data from ref. 14

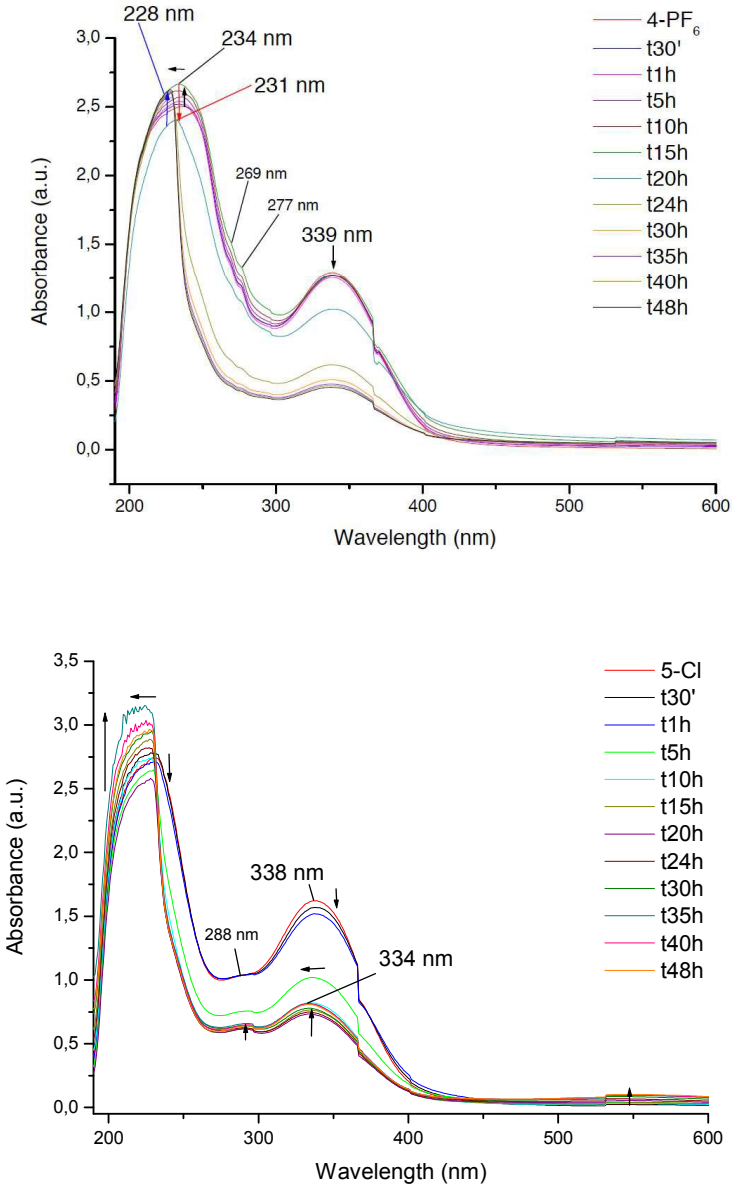

Figure 2. UV-Vis absorption spectral profiles of compounds **4-PF$_6$** and **5-Cl** in 10^{-4} M phosphate buffered solution (10 mM, pH 7.4). Spectra were recorded at different times over 48 hours at 37 °C.

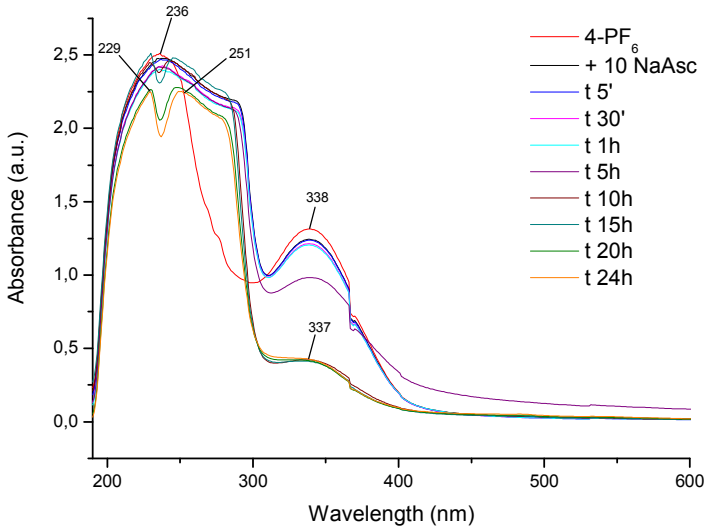

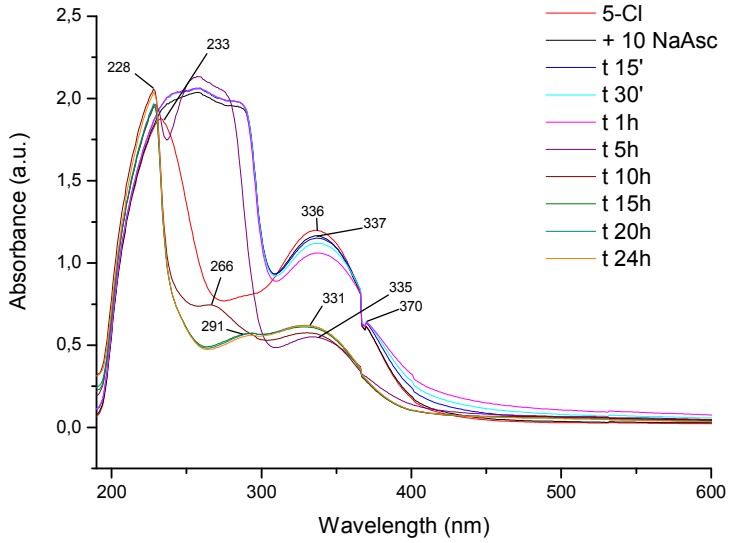

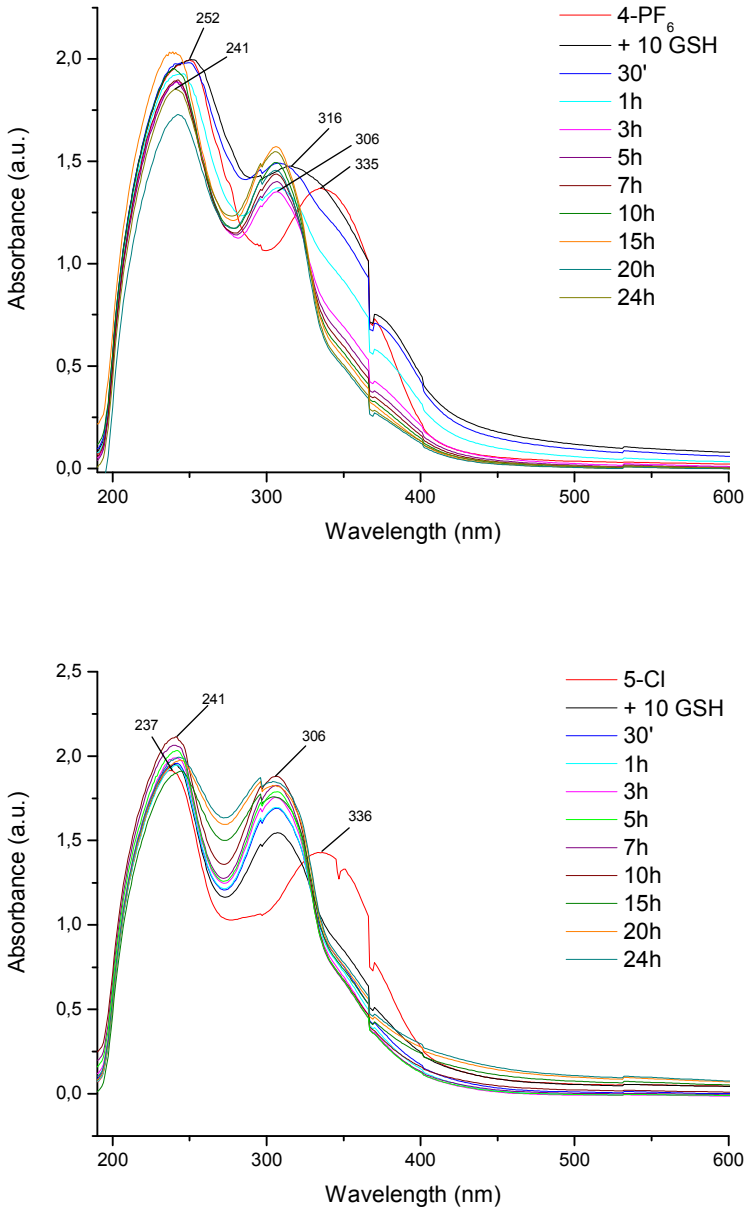

Figure 3. UV-Vis absorption spectral profiles of compounds **4-PF$_6$** and **5-Cl** in 10^{-4} M phosphate buffered solution (10 mM, pH 7.4) before and after addition of NaAsc and GSH. Spectra were recorded at different times over 24 hours at 37 °C.

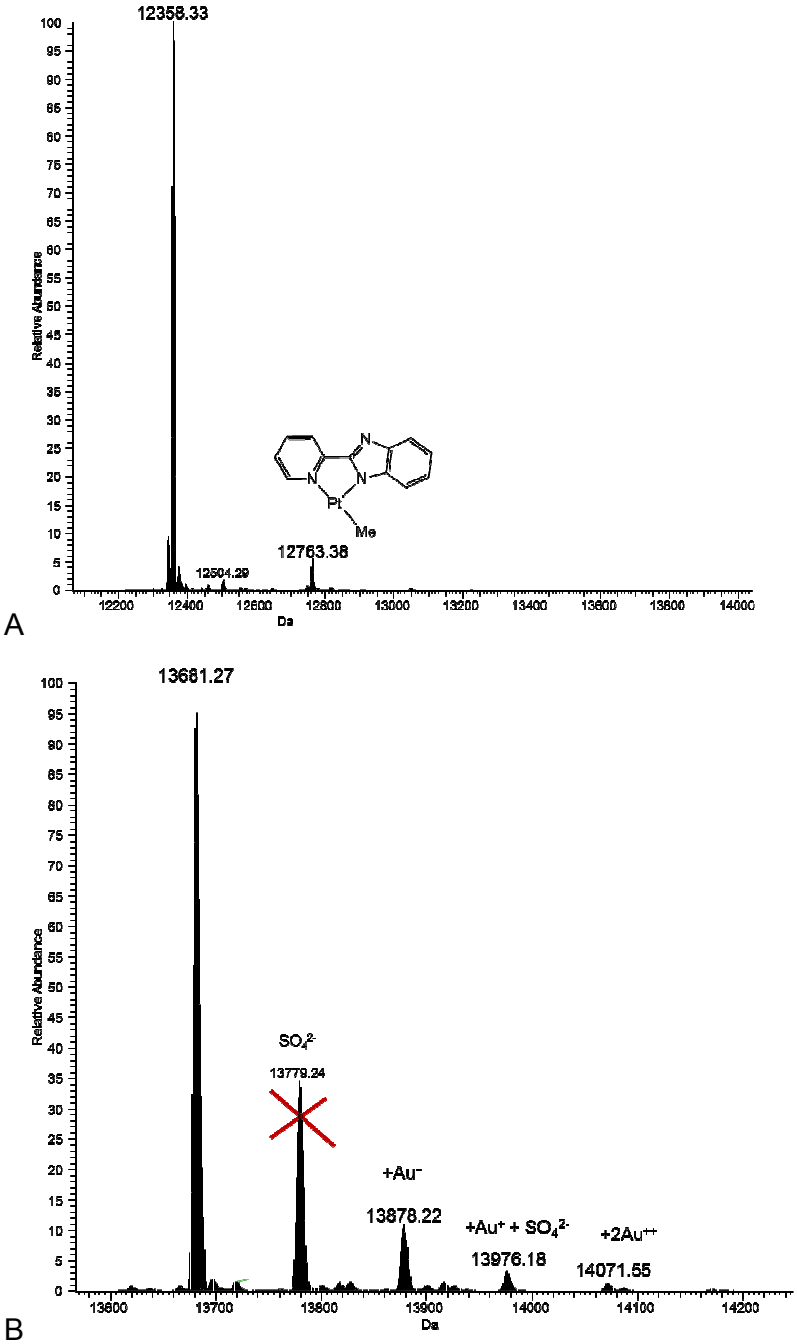

Figure 4. Deconvoluted LTQ-Orbitrap ESI mass spectra of compound **4-PF_6** in the presence of cytochrome c (A) and RNase (B) with a metallodrug-protein molar ratio of 3:1.

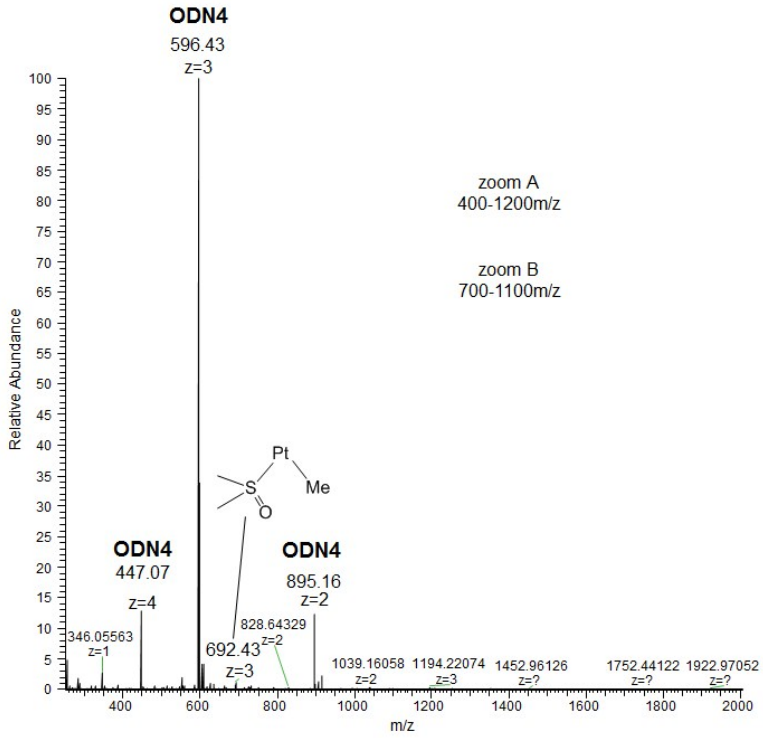

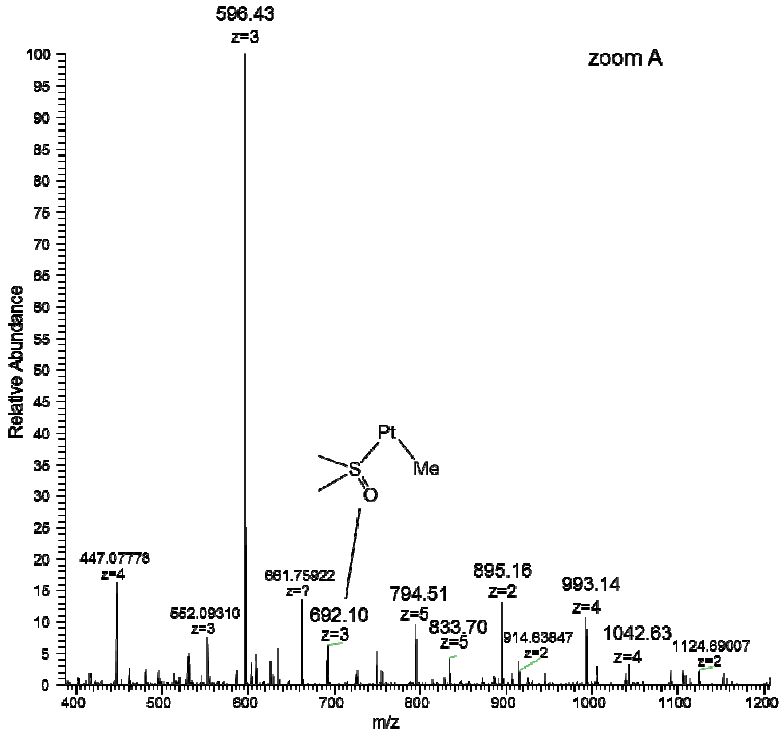

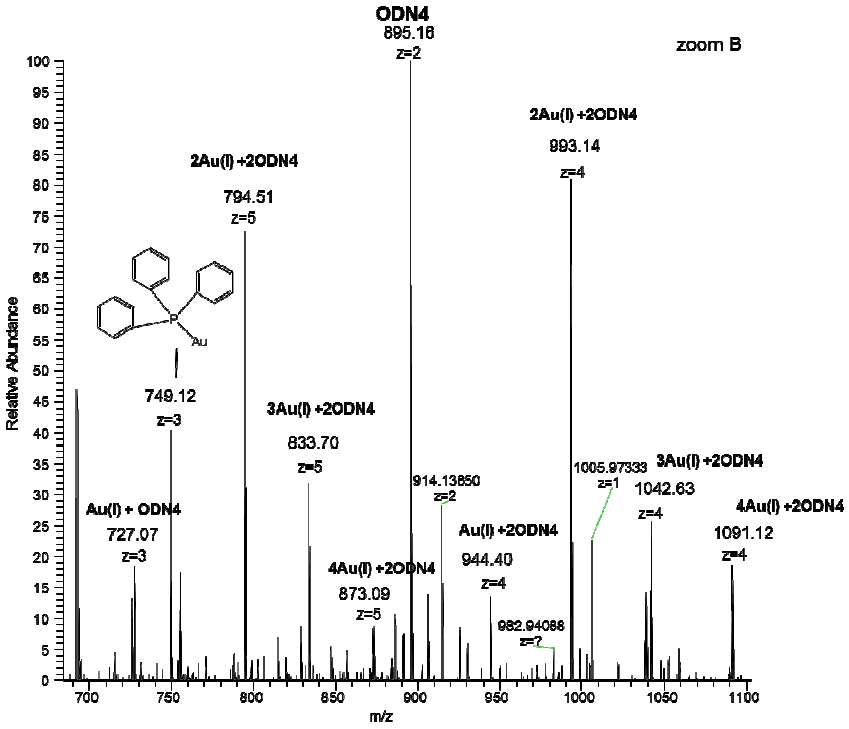

Figure 5. LTQ-Orbitrap ESI mass spectra of **4-PF$_6$** in the presence of ODN4 with a metallodrug-oligonucleotide molar ratio of 3:1

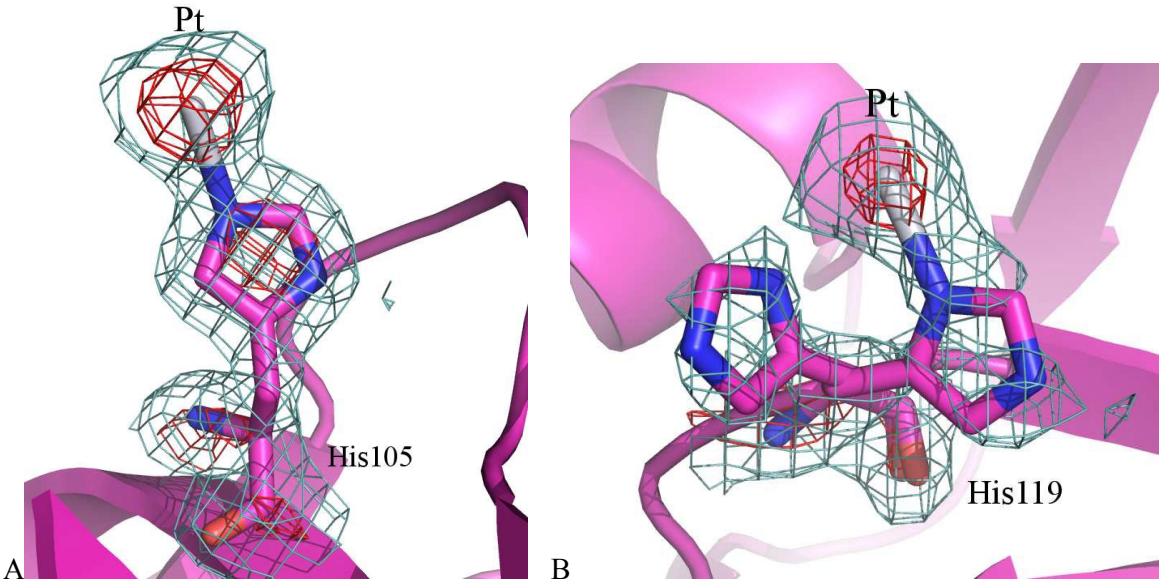

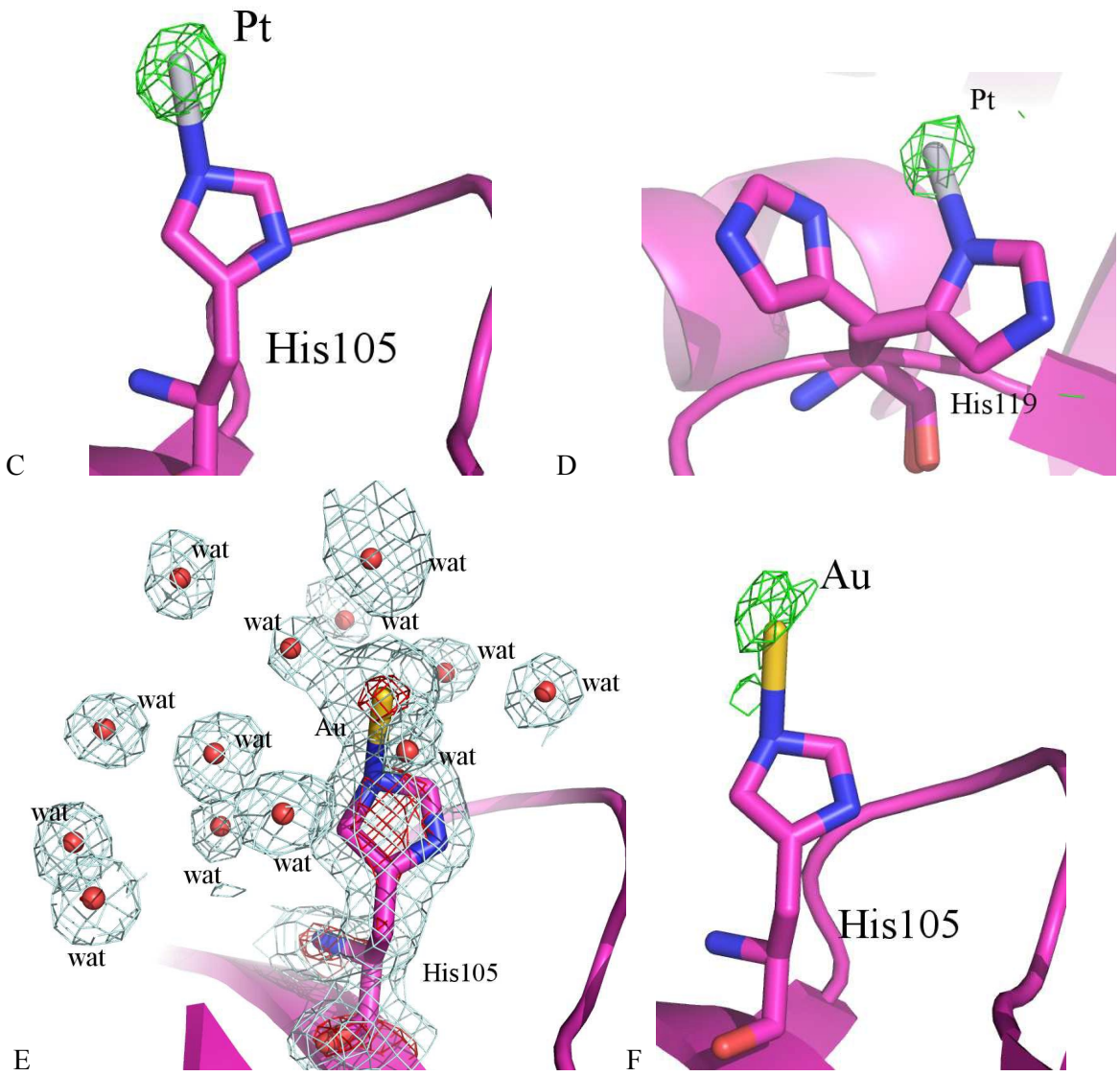

Figure 6. Details of the metal binding sites in the RNase A/**3** and RNase A/**4-PF$_6$** adducts. Pt ion is bound to His105 (panels A and C) and His119 (panels B and D) side chains in the molecule A of RNase A/**3** (panels A-D), whereas a Au ion is bound to His105 side chain in molecule A of RNase A/**4-PF$_6$** (panels E-F). In panels A, B and E 2Fo–Fc electron density maps are contoured at 1.0σ level (cyan) and 3.5σ level (red). In panel C, D and F anomalous electron density map (green) is contoured at 3.0σ level. Close to the Au binding site, the interpretation of the electron density map of possible Au ligands is complicated by the presence of a number of well-structured water molecules, which are modeled as alternative (with occupancy 0.7) to the metal (occupancy 0.3).

Graphical Abstract

Cytotoxic Properties of a New Organometallic Platinum(II) Complex and its Gold(I) Heterobimetallic Derivatives

Maria Serratrice,[a] Laura Maiore,[a] Antonio Zucca,[a,b] Sergio Stoccoro,[a,b] Ida Landini,[c] Enrico Mini,[c] Lara Massai,[d] Giarita Ferraro,[e] Antonello Merlino,[e,f] Luigi Messori*[d] and Maria Agostina Cinellu,*[a,b]

[a]*Department of Chemistry and Pharmacy, University of Sassari, via Vienna 2, 07100 Sassari, Italy. E-mail: cinellu@uniss.it*

[b]*CIRCC, Consorzio Interuniversitario Reattività Chimica e Catalisi, Università di Bari, Via Celso Ulpiani 27, 70126 Bari, Italy*

[c]*Department of Health Sciences, Section of Clinical Pharmacology and Oncology, University of Florence, viale Pieraccini 6, 50139 Firenze, Italy*

[d]*Laboratory of Metals in Medicine, Department of Chemistry, University of Florence, via della Lastruccia 3, 50019 Sesto Fiorentino, Florence, Italy. E-mail: luigi.messori@unifi.it*

[e]*Department of Chemical Sciences, University of Naples Federico II, via Cintia, 80126, Napoli, Italy.*

[f]*CNR Institute of Biostructures and Bioimges, Via Mezzocannone 16, 80100, Napoli, Italy.*

The high antiproliferative effects of a new organoplatinum(II) complex are further enhanced upon coordination of a gold(I) phosphane moiety.